Article:
Zhou, T., Silva, J., Bertling, K. et al. (Accepted: 2026) Passive beam shaping for terahertz quantum cascade lasers. IEEE Transactions on Terahertz Science and Technology. ISSN: 2156-342X (In Press)

https://doi.org/10.1109/TTHZ.2026.3667748

Passive beam shaping for terahertz quantum cascade lasers

Tao Zhou*, Jorge Silva*, Karl Bertling*, *Member, IEEE* Xiaoqiong Qi*, *Member, IEEE* Tim Gillespie*, Jari Torniainen*, Andrew Leslie*, Jeremy Herbert *, Bent Kirkeby*, Ethan Ngo*, Dragan Indjin†, Paul Dean†, Alexander Valavanis†, Lianhe Li†, Edmund H. Linfield†, A. Giles Davies†, and Aleksandar D. Rakić*, *Senior Member, IEEE*

*School of Electrical Engineering and Computer Science, The University of Queensland, Brisbane, QLD 4072 Australia

†School of Electronic and Electrical Engineering, University of Leeds, Leeds LS2 9JT UK

***Abstract*—We report the design and experimental demonstration of a passive beam-shaping module integrated into a terahertz (THz) imaging system. THz QCLs inherently produce highly divergent beams, posing challenges for beam shaping and system integration. The proposed module, comprising a feedhorn, a standard waveguide, and a transmitting horn antenna, was optimized using electromagnetic simulations to minimize coupling loss while achieving favorable far-field beam characteristics. Sensitivity analyses quantified the impact of fabrication and alignment tolerances. Far-field measurements confirm the generation of a low-divergence, single-lobe Gaussian beam, supporting high-resolution THz imaging and extending the utility of QCL-based systems to applications including biomedical diagnostics, security screening, and non-destructive testing.**

***Index Terms*—Terahertz (THz) imaging, quantum-cascade laser (QCL), Gaussian beam, Antenna simulation, Beam shaping, Terahertz beam measurement.**

I. Introduction

OVER the past two decades, terahertz (THz) imaging has gained increasing attention due to its unique capabilities in non-destructive evaluation, biomedical diagnostics, security screening, and quality control across a wide range of industries [1]–[4]. THz radiation can penetrate many dielectric materials that are opaque to visible light—such as clothing, packaging materials, or biological tissues—while remaining non-ionizing and biologically safe. These properties, and the ability to capture spectral fingerprints in the THz domain, make THz imaging highly attractive for applications requiring both spatial resolution and molecular sensitivity [5]–[7].

Manuscript received; revised. This work has been supported by the Australian Government Department of Industry, Science and Resources Critical Technologies Challenge Program (CTCF000040), the Australian National Health and Medical Research Council (NHMRC Development grant 2039614), Australian Government Department of Education through Australia's Economic Accelerator Program (IG240100515); Engineering and Physical Sciences Research Council (EP/J002356/1, EP/P021859/1, EP/W028921/1); UK Research and Innovation (Future Leader Fellowship MR/S016929/1, MR/Y011775/1) (Corresponding author: Aleksandar D. Rakić)

Tao Zhou, Jorge Silva, Karl Bertling, Xiaoqiong Qi, Tim Gillespie, Jari Torniainen, Andrew Leslie, Jeremy Herbert, Bent Kirkeby, Ethan Ngo and Aleksandar D. Rakić are with the School of Electrical Engineering and Computer Science, The University of Queensland, Brisbane, QLD 4072 Australia.(e-mail: a.rakic@uq.edu.au).

Dragan Indjin, Paul Dean, Alexander Valavanis, Lianhe Li, Edmund H. Linfield and A. Giles Davies are with the School of Electronic and Electrical Engineering, The University of Leeds, LS2 9JT Leeds, U.K.

Quantum cascade lasers (QCLs) have become indispensable sources for compact THz imaging systems due to their narrow linewidths, high spectral coherence, and growing power output capabilities combined with high-speed modulation capabilities [8]. Since their first demonstration in the mid-infrared [9], QCL technology has progressed rapidly, culminating in the realization of THz-frequency QCLs operating in the range of 1.2–5.7 THz [10]–[12]. Contemporary THz QCLs deliver pulsed peak powers of 2.4 W and are capable of continuous-wave operation at cryogenic temperatures, rendering them suitable for high-resolution imaging applications [13]. Among the waveguide architectures developed for THz QCLs, surface–plasmon (SP) and double–metal (DM) waveguides have emerged as the two dominant configurations, each offering a distinct trade-off between optical confinement, thermal management, and beam quality. The SP waveguides confine the optical mode at the interface between a top metal contact and a thin, highly doped semiconductor layer, allowing part of the field to leak into the substrate. This design yields a relatively low confinement factor ($\Gamma \approx 0.2$–0.5), but benefits from reduced overlap with lossy doped regions, resulting in low waveguide losses ($\alpha_w \sim 3$–$5\ \mathrm{cm}^{-1}$). The facet reflectivity remains moderate ($R \sim 0.3$), leading to higher mirror losses ($\alpha_m \sim 4.5$–$7.5\ \mathrm{cm}^{-1}$) [11], yet enabling efficient out-coupling and low beam divergence ($\sim 30^\circ$). In contrast, DM waveguides confine the mode between two metallic layers, achieving nearly unity confinement ($\Gamma \approx 1$), which results in elevated waveguide losses ($\alpha_w \sim 10$–$20\ \mathrm{cm}^{-1}$) due to stronger mode overlap with metal interfaces [14], [15]. Despite their large intrinsic beam divergence ($\sim 60^\circ$) and limited out-coupling per pass (5–20%), DM waveguides offer superior thermal performance—particularly with Cu–Cu bonding, reducing thermal resistance by up to 40%—and are preferred at $T > 100\,\mathrm{K}$ operation or continuous-wave operation [11]. Thus, the choice between SP and DM waveguides involves balancing beam quality and out-coupling efficiency against thermal robustness and optical confinement.

While QCLs offer unmatched compactness and spectral brightness in the terahertz regime, their beam profiles present notable challenges for system integration and imaging fidelity. For instance, SP waveguide geometries, commonly used due to their reduced waveguide loss and efficient out-coupling

compared to double-metal designs [16]. However, a persistent limitation of SP QCLs is still the poor beam quality of their free-space emission. Owing to subwavelength waveguide cross-sections and the modal content of ridge geometries, the output typically exhibits large divergence and complex, non-Gaussian far-fields characterized by dual-lobed patterns, pronounced sidelobes, and ring-like interference fringes originating from diffraction at ridge sidewalls and discontinuities at the substrate interface [11], [16]–[20]. These characteristics hinder efficient coupling into collimating optics, degrade spatial resolution in imaging systems, curtail usable working distance, and complicate optical alignment effects that are especially problematic in cryogenic and vacuum-based environments [17], [18].

Numerous beam-shaping approaches have been explored to address these challenges. First, intracavity or tightly integrated cavity-coupled schemes aim to generate improved beam quality within the laser itself, for example by using distributed-feedback gratings [21], patch-array antennas [22], and external-cavity/metasurface coupling [23]. Second, post-emission optical conditioning of the output beam, most notably by integrating hyperhemispherical silicon lenses directly onto the laser facet, can collimate the emitted beam [24], [25]. However, refractive optics at THz frequencies typically require sub-millimetre tolerances in lateral and axial position as well as tip–tilt, which may render optical coupling highly sensitive to minor mechanical perturbations not suitable for laser in a cryostat. Under cryogenic operation, precise alignment is further complicated: differential thermal contraction, constrained access, and stringent heat-load limits may collectively impede reliable positioning. Moreover, the working distances and clear apertures demanded by these lenses are often not readily compatible with RF electronics and associated packaging constraints. An interesting approach was taken in [26] where two Si lenses and a Si wafer-piece with a pinhole in a gold layer deposited on it act as a spatial filter. The effectiveness of this approach depends markedly on the collimation level of the input beam and is quite common in bulk optical systems. Photonic and antenna-based solutions adapted from microwave engineering have been implemented frequently, including planar horn structures, [27] Vivaldi antennas, [28] and metallic tapers [29], which may offer compact, lithography-compatible routes to improved directivity without recourse to macroscopic refractive elements. These techniques have shown improvements in output power and beam profile but often involve complex fabrication processes or are sensitive to positioning errors.

To overcome the limitations of these prior approaches, recent studies have demonstrated the use of passive waveguide modules that incorporate horn antennas, which reshape and guide the laser beam into more desirable far-field patterns. For example, improved beam quality and output power were demonstrated by indium-soldering a terahertz QCL into a precision-machined rectangular waveguide terminated with a diagonal horn, enabling better mode matching and reduced beam divergence. [30] Building on this concept, subsequent studies developed more sophisticated waveguide-horn assemblies that were directly integrated into compact QCL modules. These designs incorporated features such as impedance-matched transitions, optimized horn geometries, and thermal management strategies, making them well-suited for practical deployment in atmospheric sensing, spectroscopy, and remote detection scenarios using different, and complementary approach to QCL beam shaping demonstrated in this article [31]–[35]. These developments, however, have primarily focused on double-metal waveguide QCLs, whose near-field characteristics differ significantly from those of SP waveguide QCLs. As such, existing modules may not efficiently couple SP QCL emission into fundamental waveguide modes or deliver the beam quality necessary for high-resolution imaging.

In this work, we address the limitations of current solutions by introducing a compact, passive beam-shaping module specifically designed for integration with a surface-plasmon (SP) waveguide QCL. The module consists of three components: a tapered feeder horn designed to match the near-field TM mode profile at the QCL facet, a 0.5 mm WM-86 standard waveguide selected to suppress higher-order mode propagation [36], and a diagonal output horn antenna engineered for low-divergence, single-lobed far-field emission. The module geometry was optimized using full-wave electromagnetic simulations to minimize coupling loss while maintaining beam fidelity across the desired frequency range. The introduction of the horn-waveguide assembly affected markedly the spectrum of the laser with only a minor impact on the threshold current.

Sensitivity analysis was conducted to quantify the robustness of the design with respect to mechanical and alignment tolerances, ensuring suitability for system-level integration. Experimental validation confirms that the module achieves Gaussian-like output beam, significantly improving the practical imaging resolution achievable in QCL-based THz systems. The proposed approach provides a scalable and fabrication-tolerant solution for THz beam control, expanding the applicability of QCL technology in demanding imaging environments.

II. System Architecture

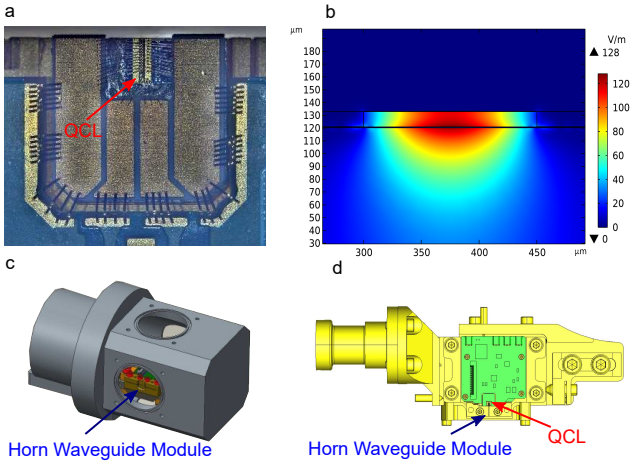

Fig. 1. (a) Top view of the surface plasmon (SP) waveguide QCL; (b) Electric field distribution evaluated at the QCL front facet; (c) 3D model of the THz QCL transceiver system mounted within a cryocooler; (d) Top-view schematic of the horn-waveguide layout.

The terahertz QCL used in our imaging system was based on a GaAs/AlGaAs heterostructure incorporating a nine-well, phonon-assisted active region design [37]. This 12 μm-thick active region was grown via solid-source molecular beam epitaxy (MBE) on a semi-insulating GaAs substrate. The active core was sandwiched between two heavily doped GaAs contact layers: a 50 nm-thick top contact and a 700 nm-thick bottom contact. Standard photolithography followed by wet chemical etching was used to define an SP ridge waveguide structure with a ridge width of 150 μm. To reduce absorption and improve thermal management, the GaAs substrate was subsequently lapped and polished down to a final thickness of 200 μm.

Two QCLs from the same wafer (L1415) were used in this study: QCL1, with a cavity length of 2.5 mm, and QCL2, with a length of 2.0 mm. Both devices were operated at 60 K, with pulsed drive currents (100 μs at 20% duty cycle) of 1.3 A for QCL1 and 0.6 A for QCL2. The corresponding peak output powers were approximately 10 mW and 6 mW, respectively, with both lasers emitting near 3.4 THz (measured as described in Ref. [38]).

In this study, we integrate the QCLs with a custom-designed passive beam-shaping module to suppress higher-order modes, reduce divergence, and deliver a single-lobe, near-Gaussian far-field pattern compatible with high-resolution THz imaging.

III. Methods

A. Experimental Design: Terahertz QCL Beam-Shaping Architecture

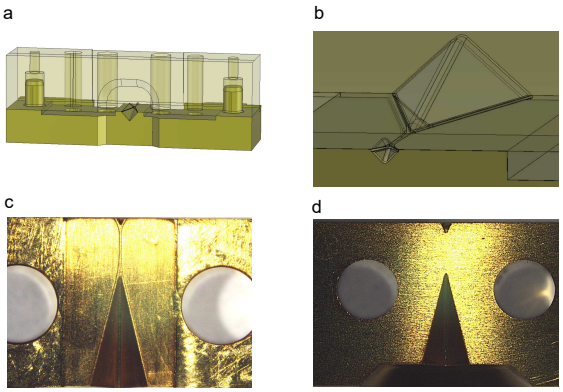

Fig. 2. Fabricated horn module: (a) Mechanical model; (b) Detail of horn apertures; (c) Top view of bottom half; (d) Top view of top half.

To overcome the intrinsic limitations of THz QCL emission, namely high beam divergence and asymmetric far-field profiles, a compact, beam-shaping module was designed and fabricated. This custom architecture was directly mounted in front of the QCL facet and served both coupling and collimation functions. The assembly comprised three main components: a receiving horn, a precision WM-86 rectangular waveguide, and a transmitting horn. Together, these elements formed an integrated transceiver unit, housed within a cryogenically cooled enclosure, as shown in Figure 1(d).

The receiving horn was designed to capture the divergent QCL emission and launch it efficiently into the waveguide. With a total length of 450 μm and an input aperture of 0.3×0.3 mm^2, it was aligned directly opposite the QCL exit facet. The horn tapered down to match the WM-86 rectangular waveguide, which has a standard internal cross-section of 86×43 μm^2, in accordance with IEEE standard 1785.1-2012 [36]. This waveguide section ensured single-mode propagation and impedance matching.

At the output end of the assembly, a 4.5 mm-long transmitting horn was employed to transform the guided mode into a well-behaved free-space beam. The transmitting horn featured an output aperture of 1.5×1.5 mm^2, optimized through electromagnetic simulations to balance beam divergence and mechanical footprint. The complete module was fabricated from gold-plated copper to ensure high conductivity, thermal stability, and compatibility with low-temperature operation.

This beam-shaping architecture enabled efficient optical coupling, reduced alignment sensitivity, and significantly improved beam symmetry and directionality, making it well-suited for imaging, sensing, and spectroscopy applications in the THz regime.

B. Modelling and Simulation of Coupling and Beam Characteristics

Full-wave electromagnetic simulations were carried out using CST Studio Suite [39] to evaluate the coupling efficiency from the QCL facet to the WM-86 rectangular waveguide, and to characterize the radiated beam from the integrated horn structure. The simulation workflow included mode excitation, S-parameter analysis (coupling and return loss), and far-field pattern extraction.

Figure 3 presents the simulated far-field beam pattern of the QCL. Here, the x-axis is defined parallel to the chip, the y-axis is defined perpendicular to the chip (in the growth direction), and the z-axis is defined along the beam-propagation direction along the ridge (normal to the emitting facet). Under the modeled conditions, the pattern is predicted to exhibit a full-width-at-half-maximum (FWHM) divergence of approximately $19^\circ \times 36^\circ$ along the x- and y-axes, respectively.

In simulation, the excitation of the dominant QCL TM_{00} mode resulted in a coupling loss of -8.5 dB with the axial standoff of 50 μm, while excitation of the first higher-order mode (TM_{01}) showed a significantly higher coupling loss of -16.5dB. This substantial difference confirms preferential coupling of the fundamental mode into the waveguide-horn assembly, which is critical for preserving beam quality and achieving efficient power delivery.

The far-field profile of the horn output demonstrates strong spatial confinement and directionality. The designed horn achieved a simulated on-axis gain of 16.8 dBi, with an FWHM beam divergence of 12.3°, and sidelobe suppression exceeding -25 dB. These characteristics indicate that the horn structure effectively transforms the highly divergent QCL emission into a narrow, symmetric, and low-sidelobe beam suitable for imaging or long-range sensing applications.

We also examined how the far-field pattern varies with the emission spectrum in order to assess spectral robustness. Our

simulations suggest that the beam-shaping module remains effective for a wide range of spectral profiles within the designed passband (2.6–3.5 THz), accommodating sources from single-mode to multimode operation. Within this range, the main-lobe formation and divergence are predicted to be relatively insensitive to spectrum, provided the spectrum lies inside the design window. These findings indicate that the approach may offer practical tolerance to device-to-device spectral variability.

Tolerance and Misalignment Sensitivity Analysis: The misalignment of the components of the horn-waveguide assembly itself has been analysed in [40]. Here we have analysed the misalignment of the horn-waveguide assembly relative to the QCL output facet. To assess the robustness of the coupling design to fabrication and assembly imperfections, a sensitivity analysis was performed using full-wave electromagnetic simulations.The excitation was based on the QCL surface plasmon mode depicted in Figure 1b. Three types of translational misalignment were considered: horizontal (x-axis), vertical (y-axis), and axial (z-axis) displacements, as illustrated in Figure 4(a–c–e). The electromagnetic simulation results confirm that the beam-shaping module demonstrates appreciable resilience to lateral misalignment. Specifically, for horizontal displacements (along the x-axis), the coupling loss remains below 0.5 dB within a tolerance window of ± 20 µm. The input for S_{21} simulation was the simulated NF distribution across the exit facet of the QCL shown in Fig. 1(b). The peak of the field distribution in Fig. 1(b) is not in the middle of the ridge and that brings about the small dip in coupled output power when the horn assembly is aligned with the centre of the ridge. The asymmetry of the facet distribution explains the results in Fig. 4(d). The results in Fig. 3 also reflect the complexity of the field distribution at the exit facet of the QCL. As the deviation increases, a gradual, monotonic rise in coupling loss is observed, reaching approximately 2.5 dB at offsets of ± 60 µm.In the vertical direction (along the y-axis), the coupling loss exhibits asymmetric sensitivity. A modest improvement of 1 dB is observed for positive displacements up to +60 µm; however, negative displacements toward -60 µm result in a more pronounced degradation, with the coupling loss rising to approximately 5 dB. This asymmetry is likely attributable to the asymmetric near-field distribution of surface plasmon QCL.

In contrast, axial displacement—defined as a gap between the QCL facet and the waveguide input—was found to be more critical. As shown in Figure 4(f), increasing the axial gap from 0 to 100 µm leads to a steady rise in coupling loss,

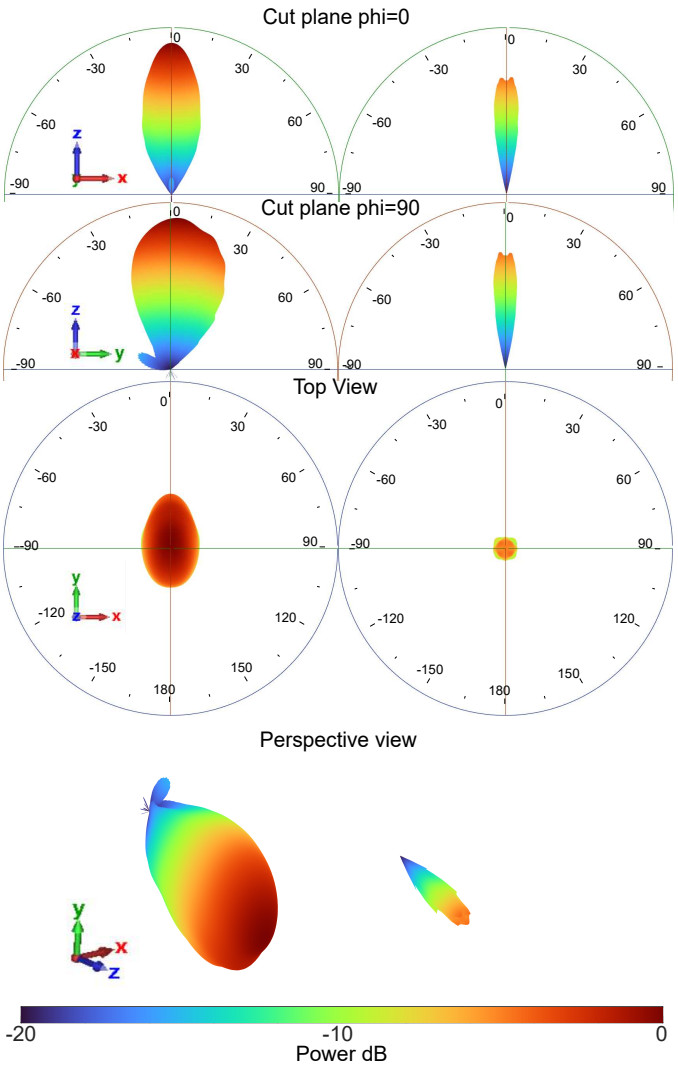

Fig. 3. Simulated far-field profiles: (left) QCL output derived from the near-field mode profile in Fig. 1(b); (right) Output of the designed transmission horn.

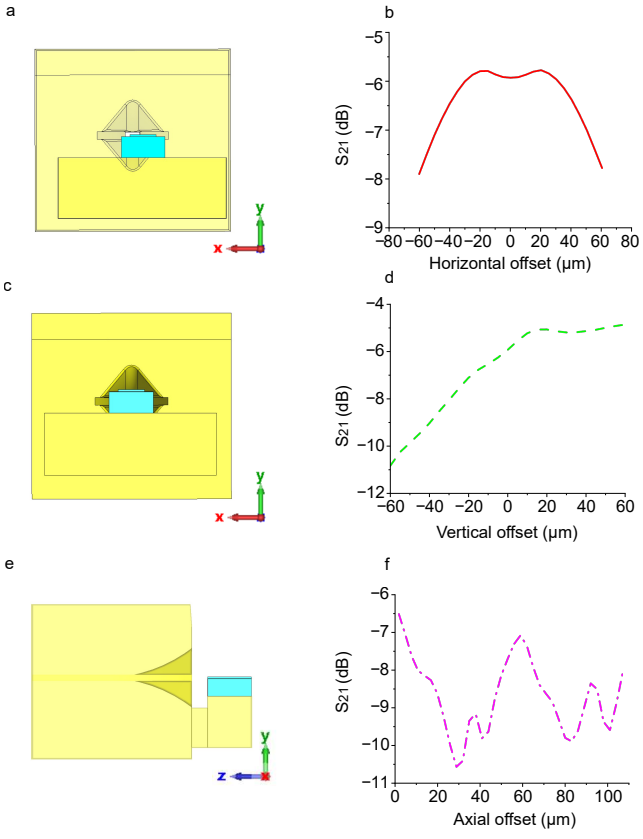

Fig. 4. Sensitivity analysis of the beam-shaping module alignment using QCL model: (a–c–e) Simulation models for horizontal, vertical, and axial displacement; (b–d–f) Corresponding coupling loss profiles.

reaching up to 4 dB. However, an optimal coupling region was identified between 50–80 µm, suggesting a non-monotonic response that may benefit from a small intentional standoff to minimize reflection or impedance mismatch.

C. Fabrication and Assembly of the Horn-Waveguide Module

The horn-waveguide module was precision-fabricated by Thomas Keating Ltd. from high-conductivity copper to provide low ohmic loss and efficient heat spreading. A thin gold overplate is applied to prevent copper oxidation, thereby maintaining low surface resistance and stable electrical contact over cryogenic cycles. The Au layer is used for chemical stability and surface durability. The mechanical design consists of two separable blocks, allowing easier access during alignment and soldering of the QCL. These blocks are aligned using precision-machined grooves and stainless steel dowel pins, ensuring repeatable positioning with a nominal machining tolerance of approximately 2 µm. This modular design simplifies fabrication while ensuring high-precision alignment of the waveguide and horn structures, which is essential for preserving beam quality and minimizing coupling loss.

IV. QCL Performance Characterization

To assess the laser performance with and without the beam-shaping module, we measured the threshold current, output power, optical spectrum, and peak operating temperature for both configurations. Figure 5 presents the pulsed light-current characteristics of QCL2 at two temperatures (60 and 70 K) where the inset shows magnified views for the horn-integrated QCL for both temperatures. Figure 6 shows the corresponding emission spectra, indicating multimode operation near 3.4 THz at 1 A bias.

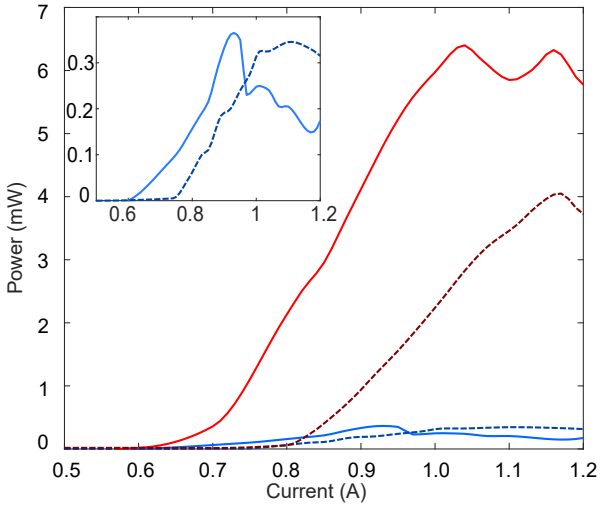

Fig. 5. Light–current (LI) characteristics of QCL2 with (blue) and without (red) the beam-shaping module. Solid curves correspond to 60 K; dashed curves to 70 K. The module is external and passive and therefore does not affect the internal thermal load or threshold current. Insets show magnified views for the horn-integrated QCL.

Integration of the beam-shaping module produced no measurable change in threshold current (remaining at approximately 0.6 A), confirming that internal loss mechanisms were not significantly affected. The peak output power fell to roughly 10% of the bare-device value. These reductions can be attributed to imperfect mode matching, propagation loss within the waveguide, and alignment tolerances at module interfaces. The spectral change (observable as the disappearance of some modes with the horn assembly in place is consistent with weak frequency-dependent feedback at the horn–waveguide interface and is consistent with observations of feedback effects on mode suppression [38].

V. Experimental Results & Analysis

The beam-shaping performance of the horn module was experimentally evaluated by measuring the far-field radiation pattern of THz QCLs, both with and without the integrated horn (in a similar way to Ref. [5]). A pyroelectric detector (model QS5-IL, Gentec-EO, Quebec, Canada), featuring a 5 mm aperture, was employed for these measurements. The detector was mounted on high-precision, motorized linear translation stage, which enabled two-dimensional spatial scanning over a 50 mm $\times$ 50 mm area located at a fixed axial distance of 42.4 mm from the QCL exit facet. No spatial filtering (e.g., pinhole) was employed in this setup. Each scan was performed at a resolution of 100 $\times$ 100 pixels.

The detector signal was amplified using a low-noise voltage preamplifier (SR560, Stanford Research Systems, California, USA) and synchronously triggered with the pulsed QCL emission using an oscilloscope (MXO44-2415, Rohde & Schwarz GmbH, Germany). Time-domain signals were acquired via a USB-6259 DAQ card (National Instruments, Texas, USA), and the QCL pulse frequency component was extracted using FFT analysis.

Figure 7 shows the measured 2D far-field beam profiles without the horn. The QCL output was highly divergent, with full width at half maximum (FWHM) beam divergences of approximately $18^\circ \times 29^\circ$ along the x- and y-axes, respectively. After integrating the horn module, the beam was transformed into a more directive, symmetric, Gaussian-like profile, clearly demonstrating the horn's effectiveness in spatial mode shaping.

With the horn, the measured FWHM beam divergence was reduced to approximately 10° along both axes, indicating a substantial improvement in beam quality. This enhancement was accompanied by a reduction in on-axis measured power incident on the detector of approximately -7 dB, consistent

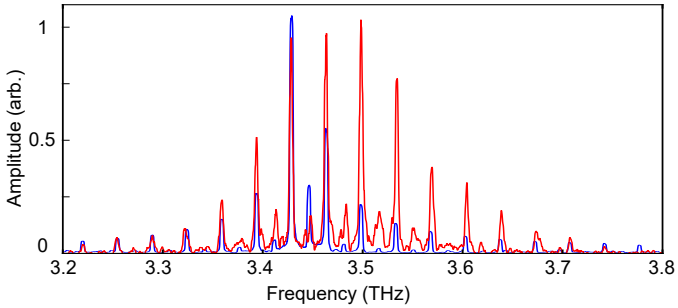

Fig. 6. Emission spectra of QCL2 with (blue) and without (red) the beam-shaping module at 60K and 1 A bias. The observed change in mode powers arise from feedback effects from the module placement.

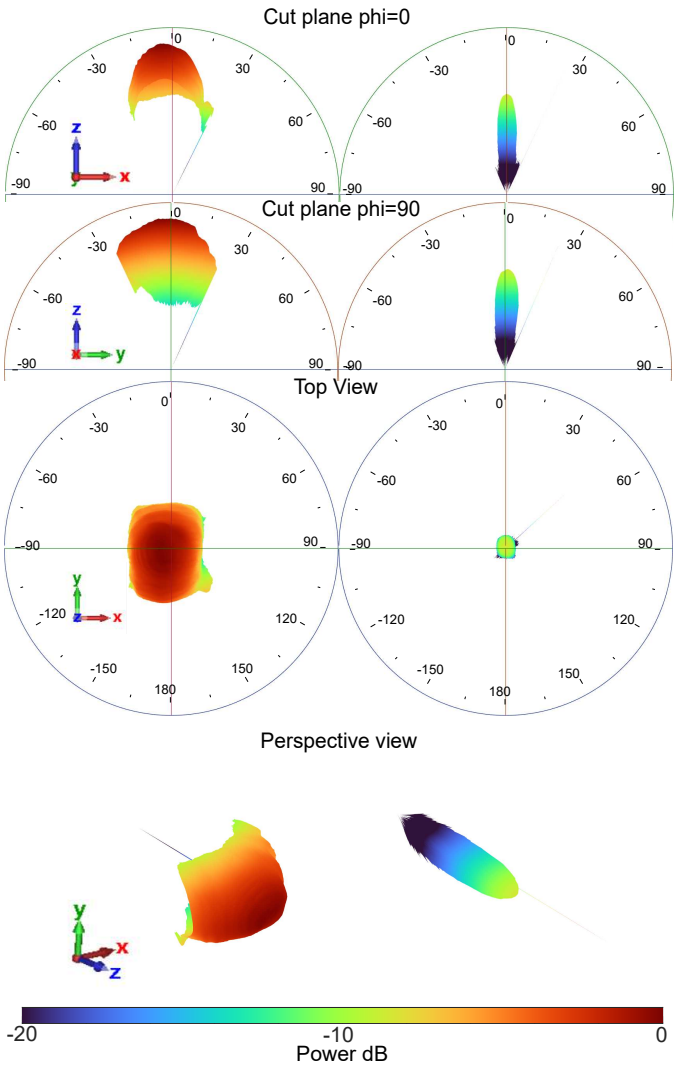

Fig. 7. Measured far-field profiles: (left) QCL1 output without horn module; (right) QCL1 output with horn-waveguide beam-shaping module.

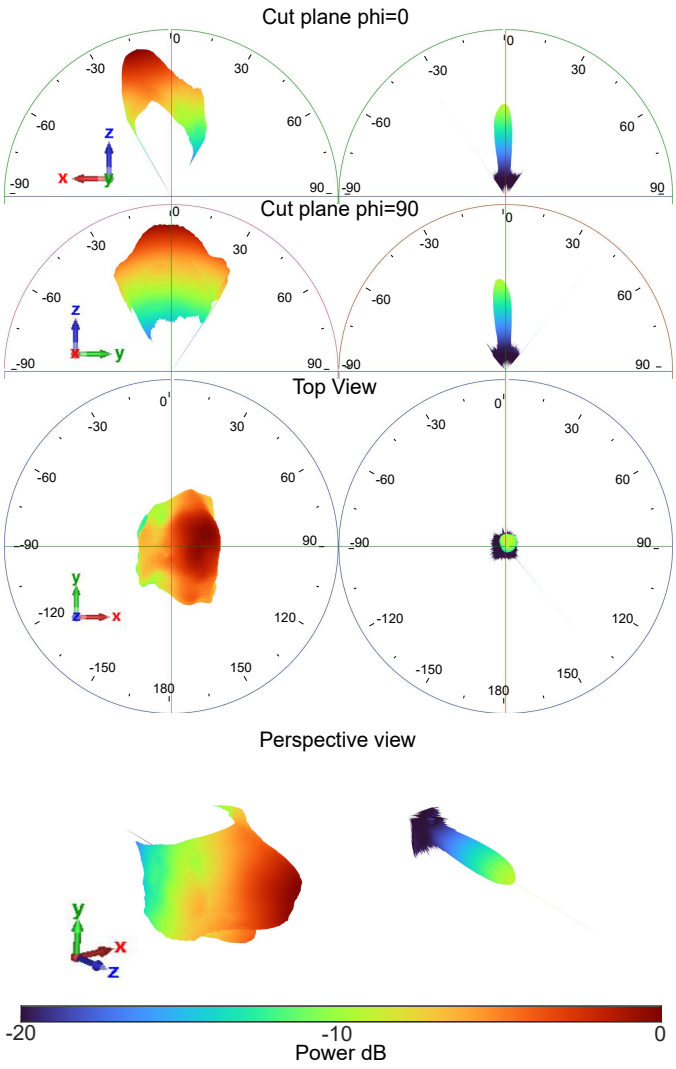

Fig. 8. Measured far-field profiles: (Left) QCL2 output without horn module; (right) QCL2 output with horn-waveguide beam-shaping module.

with simulated coupling losses and expected sensitivity to misalignment between the horn and the QCL facet. While this attenuation is non-negligible, the significant gains in spatial coherence and beam symmetry justifies the trade-off.

The change in on-axis detected power (as measured by the detector located on the optical axis of the system) was determined as the difference between the between the measured output power of the bare QCL and the QCL with the horn assembly inserted. One needs to keep in mind that we are using a finite-size aperture to measure the radiated power (5 mm diameter). Therefore the insertion loss is conflated with the reduced FWHM divergence of the beam. This explains the differences between the simulation and the experiment.

To evaluate the robustness of the horn design, a second horn module was tested with a different THz QCL, which exhibited an FWHM beam divergence of $19^\circ \times 30.5^\circ$ along the x- and y-axes, respectively, and a multi-lobed emission profile with a prominent off-axis main lobe. As shown in Figure 8, the horn assembly effectively suppressed secondary lobes and reduced beam divergence, producing a clean, centrally aligned, single-lobed output. A reduction in on-axis detected power of approximately -8.5 dB and a reduced FWHM divergence of 11.7° were observed. These results confirm the consistency and reliability of the horn design across QCLs with differing native emission profiles.

VI. Conclusions

This work presents the design, modeling, fabrication, and experimental validation of a compact, passive beam-shaping module for THz QCL imaging systems. A custom-designed horn–waveguide–horn module was integrated directly onto the QCL facet, enabling improved far-field beam control without requiring internal modifications to the laser cavity.

Finite-element modeling in CST Studio Suite guided the design optimization, with simulations showing strong fundamental mode coupling, high forward gain, and suppressed sidelobe radiation. The simulated coupling loss between the QCL and WM-86 standard waveguide was approximately -8.5 dB for the fundamental TM_{00} mode, while higher-order modes were effectively attenuated. Sensitivity analyses identified fabrication and assembly tolerances for robust performance.

Experimental validation using a pyroelectric detector confirmed that the integrated module significantly improved the far-field beam profile, transforming divergent or multi-lobed emission into a symmetric, single-lobed Gaussian beam with divergence angles of approximately 10° (QCL1) and 12° (QCL2) along both lateral axes. These results were in close agreement with simulation predictions. The beam shaping introduced a reduction of on-axis power of −7 dB (QCL1) and −8.5 dB (QCL2), consistent with change in FWHM of the beam, modeled coupling losses, surface roughness, and accounting for minor misalignment between the feed horn and the QCLs.

Regarding scope and applicability, this approach is expected to be applicable to DM geometries. It is essential to note that the beam-shaping module is external and passive; therefore, it does not alter the internal thermal performance of the laser. For SP devices, owing to their larger lateral mode expansion, the beam shaping module often benefits from a modest increase in module–facet standoff to maintain outcoupling efficiency. By contrast, for DM devices, the sub-wavelength exit aperture and strong vertical confinement tend to produce high initial divergence and a heightened susceptibility to facet back-reflection. In this case, mode mismatch is generally more severe than for SP devices, so coupling loss is expected to be comparable to, or somewhat higher than, the SP cases.

This work demonstrates a practical and manufacturable solution for achieving collimated, low-divergence beams from surface plasmon QCLs, an essential requirement for high-resolution THz imaging applications. The modular design and tolerance-resilient assembly further support scalability across multiple devices.

VII. Data Availability

The data associated with this work is freely available at https://doi.org/10.48610/a02ef1c

References

[1] X. Chen, H. Lindley-Hatcher, R. I. Stantchev, J. Wang, K. Li, A. Hernandez Serrano, Z. D. Taylor, E. Castro-Camus, and E. Pickwell-MacPherson, "Terahertz (thz) biophotonics technology: Instrumentation, techniques, and biomedical applications," *Chemical Physics Reviews*, vol. 3, no. 1, 2022.

[2] A. Rakić, T. Taimre, K. Bertling, Y. Lim, P. Dean, A. Valavanis, and D. Indjin, "Sensing and imaging using laser feedback interferometry with quantum cascade lasers," *Applied Physics Reviews*, vol. 6, no. 2, 2019.

[3] J.-H. Son, S. J. Oh, and H. Cheon, "Potential clinical applications of terahertz radiation," *Journal of Applied Physics*, vol. 125, no. 19, 2019.

[4] A. G. Markelz and D. M. Mittleman, "Perspective on terahertz applications in bioscience and biotechnology," *Acs Photonics*, vol. 9, no. 4, pp. 1117–1126, 2022.

[5] J. Silva, M. Plöschner, K. Bertling, M. Ghantala, T. Gillespie, J. Torniainen, J. Herbert, Y. L. Lim, T. Taimre, X. Qi *et al.*, "Subwavelength 3d terahertz imaging with a single-pixel laser transceiver," *Optics Express*, vol. 33, no. 10, pp. 21 938–21 950, 2025.

[6] X. Qi, K. Bertling, J. Torniainen, F. Kong, T. Gillespie, C. Primiero, M. Stark, P. Dean, D. Indjin, L. Li *et al.*, "Terahertz in vivo imaging of human skin: Toward detection of abnormal skin pathologies," *APL bioengineering*, vol. 8, no. 1, 2024.

[7] M. Kashyap, J. Torniainen, K. Bertling, U. Kundu, K. Singh, B. C. Donose, T. Gillespie, Y. L. Lim, D. Indjin, L. Li *et al.*, "Coherent terahertz laser feedback interferometry for hydration sensing in leaves," *Optics Express*, vol. 31, no. 15, pp. 23 877–23 888, 2023.

[8] G. Agnew, A. Grier, T. Taimre, Y. Lim, M. Nikolić, A. Valavanis, J. Cooper, P. Dean, S. Khanna, M. Lachab *et al.*, "Efficient prediction of terahertz quantum cascade laser dynamics from steady-state simulations," *Applied Physics Letters*, vol. 106, no. 16, 2015.

[9] J. Faist, F. Capasso, D. L. Sivco, C. Sirtori, A. L. Hutchinson, and A. Y. Cho, "Quantum cascade laser," *Science*, vol. 264, no. 5158, pp. 553–556, 1994.

[10] R. Köhler, A. Tredicucci, F. Beltram, H. E. Beere, E. H. Linfield, A. G. Davies, D. A. Ritchie, R. C. Iotti, and F. Rossi, "Terahertz semiconductor-heterostructure laser," *nature*, vol. 417, no. 6885, pp. 156–159, 2002.

[11] M. S. Vitiello and A. Tredicucci, "Physics and technology of terahertz quantum cascade lasers," *Advances in Physics: X*, vol. 6, no. 1, p. 1893809, 2021.

[12] M. Shahili, S. J. Addamane, A. D. Kim, C. A. Curwen, J. H. Kawamura, and B. S. Williams, "Continuous-wave gaas/algaas quantum cascade laser at 5.7 thz," *Nanophotonics*, vol. 13, no. 10, pp. 1735–1743, 2024.

[13] L. Li, L. Chen, J. Freeman, M. Salih, P. Dean, A. Davies, and E. Linfield, "Multi-watt high-power thz frequency quantum cascade lasers," *Electronics Letters*, vol. 53, no. 12, pp. 799–800, 2017.

[14] B. S. Williams, "Terahertz quantum-cascade lasers," *Nature photonics*, vol. 1, no. 9, pp. 517–525, 2007.

[15] G. Scalari, M. I. Amanti, C. Walther, R. Terazzi, M. Beck, and J. Faist, "Broadband thz lasing from a photon-phonon quantum cascade structure," *optics Express*, vol. 18, no. 8, pp. 8043–8052, 2010.

[16] M. Hajenius, P. Khosropanah, J. Hovenier, J. Gao, T. Klapwijk, S. Barbieri, S. Dhillon, P. Filloux, C. Sirtori, D. Ritchie *et al.*, "Surface plasmon quantum cascade lasers as terahertz local oscillators," *Optics letters*, vol. 33, no. 4, pp. 312–314, 2008.

[17] E. Bründermann, M. Havenith, G. Scalari, M. Giovannini, J. Faist, J. Kunsch, L. Mechold, and M. Abraham, "Turn-key compact high temperature terahertz quantum cascade lasers," *Optics Express*, vol. 14, no. 5, pp. 1829–1841, 2006.

[18] H. Richter, M. Greiner-Bär, S. Pavlov, A. Semenov, M. Wienold, L. Schrottke, M. Giehler, R. Hey, H. Grahn, and H.-W. Hübers, "A compact, continuous-wave terahertz source based on a quantum-cascade laser and a miniature cryocooler," *Optics express*, vol. 18, no. 10, pp. 10 177–10 187, 2010.

[19] H.-W. Hübers, S. Pavlov, A. Semenov, R. Köhler, L. Mahler, A. Tredicucci, H. Beere, D. Ritchie, and E. Linfield, "Terahertz quantum cascade laser as local oscillator in a heterodyne receiver," *Optics express*, vol. 13, no. 15, pp. 5890–5896, 2005.

[20] M. Salih, P. Dean, A. Valavanis, S. Khanna, L. Li, J. Cunningham, A. Davies, and E. Linfield, "Terahertz quantum cascade lasers with thin resonant-phonon depopulation active regions and surface-plasmon waveguides," *Journal of Applied Physics*, vol. 113, no. 11, 2013.

[21] M. I. Amanti, M. Fischer, G. Scalari, M. Beck, and J. Faist, "Low-divergence single-mode terahertz quantum cascade laser," *Nature Photonics*, vol. 3, no. 10, pp. 586–590, 2009.

[22] L. Bosco, C. Bonzon, K. Ohtani, M. Justen, M. Beck, and J. Faist, "A patch-array antenna single-mode low electrical dissipation continuous wave terahertz quantum cascade laser," *Applied Physics Letters*, vol. 109, no. 20, 2016.

[23] L. Xu, C. A. Curwen, P. W. Hon, Q.-S. Chen, T. Itoh, and B. S. Williams, "Metasurface external cavity laser," *Applied Physics Letters*, vol. 107, no. 22, 2015.

[24] A. Wei Min Lee, Q. Qin, S. Kumar, B. S. Williams, Q. Hu, and J. L. Reno, "High-power and high-temperature thz quantum-cascade lasers based on lens-coupled metal–metal waveguides," *Optics letters*, vol. 32, no. 19, pp. 2840–2842, 2007.

[25] R. Degl'Innocenti, Y. Shah, D. Jessop, Y. Ren, O. Mitrofanov, H. Beere, and D. Ritchie, "Hollow metallic waveguides integrated with terahertz quantum cascade lasers," *Optics Express*, vol. 22, no. 20, pp. 24 439–24 449, 2014.

[26] Y. Gan, B. Mirzaei, S. van der Poel, J. R. Silva, M. Finkel, M. Eggens, M. Ridder, A. Khalatpour, Q. Hu, F. van der Tak *et al.*, "3.9 thz spatial filter based on a back-to-back si-lens system," *Optics Express*, vol. 28, no. 22, pp. 32 693–32 708, 2020.

[27] F. Wang, I. Kundu, L. Chen, L. Li, E. H. Linfield, A. G. Davies, S. Moumdji, R. Colombelli, J. Mangeney, J. Tignon *et al.*, "Engineered far-fields of metal-metal terahertz quantum cascade lasers with integrated planar horn structures," *Optics express*, vol. 24, no. 3, pp. 2174–2182, 2016.

[28] U. Senica, E. Mavrona, T. Olariu, A. Forrer, M. Shahmohammadi, M. Beck, J. Faist, and G. Scalari, "An antipodal vivaldi antenna for improved far-field properties and polarization manipulation of broadband

terahertz quantum cascade lasers," *Applied Physics Letters*, vol. 116, no. 16, p. 161105, 2020.
[29] T. Akalin, J.-F. Lampin, E. Peytavit, S. Barbieri, W. Maineult, C. Sirtori, J. Alton, H. E. Beere, and D. Ritchie, "Qcl with terahertz tem-horn antennas," in *2007 Joint 32nd International Conference on Infrared and Millimeter Waves and the 15th International Conference on Terahertz Electronics*. IEEE, 2007, pp. 474–475.
[30] A. Valavanis, M. Henry, Y. Han, O. Auriacombe, R. Dong, T. Rawlings, L. Li, M. Oldfield, N. Brewster, A. Davies *et al.*, "Feedhorn-integrated thz qcl local oscillators for the locus atmospheric sounder," in *2016 41st International Conference on Infrared, Millimeter, and Terahertz waves (IRMMW-THz)*. IEEE, 2016, pp. 1–2.
[31] M. Justen, K. Otani, D. Turčinková, F. Castellano, M. Beck, U. U. Graf, D. Büchel, M. Schultz, and J. Faist, "Waveguide embedding of a double-metal 1.9-thz quantum cascade laser: Design, manufacturing, and results," *IEEE Transactions on Terahertz Science and Technology*, vol. 7, no. 5, pp. 609–613, 2017.
[32] B. Ellison, A. Valavanis, O. Auriacombe, D. Gerber, T. Rawlings, N. Brewster, M. Oldfield, Y. Han, L. Li, E. Zafar *et al.*, "3.5 thz quantum-cascade laser emission from dual diagonal feedhorns," *International Journal of Microwave and Wireless Technologies*, vol. 11, no. 9, pp. 909–917, 2019.
[33] E. Nuttall, Y. Han, D. Pardo, S. S. Kondawar, N. Brewster, M. Salih, L. Li, M. D. Horbury, A. G. Davies, E. H. Linfield *et al.*, "Waveguide integration of a> 4.7-thz quantum-cascade laser," *Electronics Letters*, vol. 59, no. 2, p. e12703, 2023.
[34] M. Salih, S. S. Kondawar, N. Brewster, L. H. Li, E. H. Linfield, H. Wang, P. G. Huggard, J. R. Freeman, D. Gerber, and A. Valavanis, "Integration of a 2.1-thz quantum cascade laser within an ieee wm-130 rectangular metallic waveguide," in *2023 48th International Conference on Infrared, Millimeter, and Terahertz Waves (IRMMW-THz)*, 2023, pp. 1–2.
[35] M. C. Ertl, D. Schock, A. Invernici, M. Giparakis, M. Jaidl, A. M. Andrews, J. Darmo, and K. Unterrainer, "Integrated metallic hollow waveguides with terahertz quantum cascade lasers," *Journal of Infrared, Millimeter, and Terahertz Waves*, vol. 47, no. 1, p. 3, 2026.
[36] IEEE Standards Association, *IEEE Standard for Rectangular Metallic Waveguides and Their Interfaces for Frequencies of 110 GHz and Above–Part 1: Frequency Bands and Waveguide Dimensions*, IEEE Std. 1, Mar. 2013, available at: https://doi.org/10.1109/IEEESTD.2013.6471987.
[37] M. Wienold, L. Schrottke, M. Giehler, R. Hey, W. Anders, and H. Grahn, "Low-voltage terahertz quantum-cascade lasers based on lo-phonon-assisted interminiband transitions," *Electronics letters*, vol. 45, no. 20, pp. 1030–1031, 2009.
[38] J. Keeley, J. Freeman, K. Bertling, Y. L. Lim, R. A. Mohandas, T. Taimre, L. H. Li, D. Indjin, A. D. Rakić, E. H. Linfield *et al.*, "Measurement of the emission spectrum of a semiconductor laser using laser-feedback interferometry," *Scientific reports*, vol. 7, no. 1, p. 7236, 2017.
[39] Dassault Systèmes, "Cst studio suite," https://www.3ds.com/products-services/simulia/products/cst-studio-suite/, 2025, accessed: 2025-01-31.
[40] D. Jayasankar, A. Koj, J. Hesler, and J. Stake, "Impact of e-plane misalignment on thz diagonal horn antennas," *IEEE Transactions on Terahertz Science and Technology*, 2024.

Jorge Silva received his M.Sc. degree in Physics from the University of Minho, Portugal, and is currently a Ph.D. candidate at The University of Queensland, Australia, under the supervision of Prof. Aleksandar D. Rakic. His research focuses on terahertz imaging and photonics, with a particular emphasis on quantum cascade laser-based systems and laser feedback interferometry for high-resolution, non-destructive 3D imaging. His work bridges fundamental optics and applied sensing, contributing to the advancement of compact and sensitive THz imaging technologies.

Karl Bertling (S'06–M'12) received his BE (Electrical Engineering) and a BSc (Physics) in 2003, a MPhil (Electrical Engineering) in 2006 and a Phd (Electrical Engineering) in 2012, all from The University of Queensland. His current research interests are imaging and sensing via laser feedback interferometry (utilizing the self-mixing effect). He has contributed to the body of knowledge for this technique in visible, near-IR, mid-IR and terahertz semiconductor lasers.

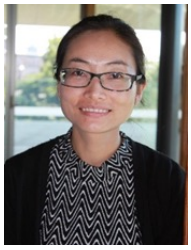

Xiaoqiong Qi received her BSc in Electrical Engineering in 2003 and her PhD in Physics in 2009, both from Lanzhou University, China. From 2007 to 2009, she conducted research at the University of California, Los Angeles (UCLA) through a joint PhD training program. She subsequently worked at the Institute of Semiconductors, Chinese Academy of Sciences, Beijing, first as a postdoctoral researcher and later as an Associate Professor. She is currently a Senior Lecturer at the University of Queensland. Her research interests include semiconductor laser dynamics in diode lasers and quantum cascade lasers, optical sensing, imaging, and spectroscopy in the near-infrared and terahertz frequency bands for biomedical applications.

Bent Kirkby is a Mechanical Design Engineer with expertise in R&D, product design, 3D CAD, prototyping, and production engineering. His work focuses on developing innovative mechanical systems using advanced manufacturing techniques, including 3D printing.

Tao Zhou received the B.Sc. degree in electrical engineering from the Northwestern Polytechnical University, China, and is currently a Ph.D. candidate at The University of Queensland, Australia, under the supervision of Prof. Aleksandar D. Rakic. His work spans the radio-frequency, microwave, and terahertz regimes by adapting principles of circuits, antennas, and wave propagation across these frequency bands. This enables the development of novel devices, RF front-end systems, and sensing platforms. His research interests include the design of antennas for terahertz quantum cascade laser imaging systems and micro-cavities for low-current terahertz QCLs.

Tim Gillespie is a professional engineer with over 24 years of experience in commercial design engineering. He is an inventor on 34 US patents and has worked on a significant number of products from initial design stage and prototyping through to production. His current research interests include the design and implementation of QCL based THz pulsed transceivers.

Jari Torniainen received the B.Sc. (tech.) and M.Sc. (tech.) degrees in electrical engineering from Aalto University, Espoo, Finland, in 2014 and 2015, and the Ph.D. degree in applied physics from the University of Eastern Finland, Joensuu, Finland, in 2020. He is specialized in biomedical signal and image analysis. His current research interests biomedical spectroscopy and spectroscopic imaging for detecting pathologies in multilayered tissues.

Andrew Leslie has graduated from the University of Southern Queensland, Australia in 2017 with a Bachelor (BENG) of Electrical and Electronic Engineering. He is also a registered Chartered Engineer (MIEAust CPEng). His experience is in hardware design with skills in commercial and defence applications.

Jeremy Herbert received his BE and PhD from The University of Queensland. He is currently a Lecturer in the School of Electrical Engineering and Computer Science at The University of Queensland. His research spans embedded systems, photonics, and electronic devices

Dragan Indjin received the B.S., M.S., and Ph.D. degrees in electrical engineering from the University of Belgrade, Serbia. He joined the Faculty of Electrical Engineering, University of Belgrade, in 1989, where he later became an Associate Professor. Since 2001, he has been with the Institute of Microwaves and Photonics, School of Electronic and Electrical Engineering, University of Leeds, Leeds, U.K., where he currently holds a position of Reader (Associate Professor) in Optoelectronics and Nanoscale Electronics. His research interests include the electronic structures, optical and transport properties, optimization and design of quantum wells, superlattices, quantum-cascade lasers, and quantum-well infrared photodetectors from near- to far- infrared and terahertz spectral ranges. He is currently focused on applications of quantum-cascade lasers and interband cascade lasers for sensing and imaging applications. Dr. Indjin was a recipient of the Prestigious Academic Fellowship from the Institute of Microwaves and Photonics, School of Electronic and Electrical Engineering, University of Leeds, in 2005. He is currently coordinator of major international projects on infrared and terahertz imaging and sensing for medical and security application.

Paul Dean received the M.Phys. (Hons.) degree in physics in 2001 and the Ph.D. degree in laser physics in 2005, both from the University of Manchester, Manchester, U.K. In 2005, he was appointed as a Post-Doctoral Research Associate at the Institute of Microwaves and Photonics, School of Electronic and Electrical Engineering, University of Leeds, Leeds, U.K. In 2011 he was awarded a Fellowship by the Engineering and Physical Sciences Research Council (UK). His current research interests include terahertz optoelectronics, quantum cascade lasers, and terahertz imaging techniques.

Alexander Valavanis received the M.Eng. (Hons.) degree in electronic engineering from the University of York, York, U.K., in 2004, and the Ph.D. degree in electronic and electrical engineering from the University of Leeds, Leeds, U.K., in 2009. He is currently an Associate Professor in terahertz instrumentation with the University of Leeds, and holds a UKRI Future Leader Fellowship. His research interests include terahertz instrumentation, quantum cascade lasers, remote sensing, gas detection, and computational methods for quantum electronics. Dr. Valavanis is a Member of the Institution of Engineering and Technology (IET).

Lianhe Li Dr. Li received his PhD degree from Institute of Semiconductors, Chinese Academy of Sciences, in 2001. From 2001 to 2003, he was with the Laboratoire de Photonique et des Nanostructures (CNRS), France, where his research interests focused on MBE growth and characterization of low bandgap GaAs-based III-V diluted nitride materials and devices. In 2003, he joined Institute of Photonics and Quantum Electronics, Ecole Polytechnique Federale de Lausanne (Switzerland), working on InAs quantum dots (QD) for 1.3-um wavelength semiconductor lasers, superluminescence light emitting diodes (SLEDs) and single photon devices. Since 2008, he has been with the school of Electronic and Electrical Engineering, University of Leeds (UK), working on the III-V semiconductor optoelectronic materials and devices (GaAs-, InP- and Sb-based) for mid-infrared and THz wave generation/detection with particular emphasis on quantum cascade lasers (QCLs), quantum cascade detectors (QCDs), quantum well infrared photodetectors (QWIPs), and type-II InAs/GaSb quantum well and superlattice.

Edmund H. Linfield received the B.A. (Hons.) degree in physics and the Ph.D. degree from the University of Cambridge, Cambridge, U.K., in 1986 and 1991, respectively.,He continued his research with the Cavendish Laboratory, University of Cambridge, becoming an Assistant Director of Research and a Fellow of Gonville and Caius College, Cambridge, U.K., in 1997. In 2004, he joined the University of Leeds, Leeds, U.K., to take up the Chair of Terahertz Electronics, where he is currently also the Director of Research and Innovation with the School of Electronic and Electrical Engineering. His research interests include semiconductor growth and device fabrication, terahertz-frequency optics and electronics, and nanotechnology. Prof. Linfield shared the Faraday Medal and Prize from the Institute of Physics in 2014, and was the recipient of the Wolfson Research Merit Award from the Royal Society in 2015.

A. Giles Davies Alexander G. Davies received the B.Sc. (Hons.) degree in chemical physics from the University of Bristol, Bristol, U.K., in 1987, and the Ph.D. degree from the University of Cambridge, Cambridge, U.K., in 1991.,In 1991, he joined the University of New South Wales, Sydney, NSW, Australia, supported by an Australian Research Council Fellowship, before returning to the Cavendish Laboratory, University of Cambridge in 1995 as a Royal Society University Research Fellow, and subsequently Trevelyan Fellow of Selwyn College, Cambridge. Since 2002, he has been with the School of Electronic and Electrical Engineering, University of Leeds, as a Professor of electronic and photonic engineering, and is currently also the Pro-Dean for Research and Innovation with the Faculty of Engineering. His research interests include the optical and electronic properties of semiconductor devices, terahertz frequency electronics and photonics, and the exploitation of biological properties for nanostructure engineering.,Prof. Davies is a Fellow of the Royal Academy of Engineering and the Institute of Physics, and both a Chartered Physicist and Chartered Engineer. He received a Wolfson Research Merit award from the Royal Society in 2011, and shared the Faraday Medal and Prize from the Institute of Physics in 2014.

Aleksandar D. Rakić (M'93–SM'10) leads the Photonics group at the School of Electrical Engineering and Computer Science, The University of Queensland, focusing on the development of technologies for sensing and imaging across the electromagnetic spectrum including microwave, terahertz wave and optical systems. Over the past 20 years Rakić group pioneered the development of several world's first laser-feedback interferometric sensors including systems based on monolithic vertical-cavity surface-emitting laser arrays (VCSELs), blue-green lasers, terahertz quantum cascade lasers and mid-infrared interband cascade lasers. His current research involves the development of sensing and imaging systems exploiting the THz spectrum for applications from security and defense to in vivo biomedical imaging. His other principal contributions relate to the design and characterization of surface-emitting optoelectronic devices (VCSELs and light emitting diodes).